

# Optimal Disturbance Rejection Control Design for Electric Power Steering Systems

N. Mehrabi, N. L. Azad, and J. McPhee.

**Abstract**— Nowadays many automobile manufacturers are switching to Electric Power Steering (EPS) for its advantages on performance and cost.

In this paper, a mathematical model of a column type EPS system is established, and its state-space expression is constructed. Then three different control methods are implemented and performance, robustness and disturbance rejection properties of the EPS control systems are investigated. The controllers are tested via simulation and results show a modified Linear Quadratic Gaussian (LQG) controller can track the characteristic curve well and effectively attenuate external disturbances.

## I. INTRODUCTION

THE Steering system is one of the major subsystems of a vehicle. As vehicles have switched to now established preference of front-wheel drive, with transversely mounted power unit, which can result in high weight concentration over steered wheels, the effort to turn the steering wheel manually is greatly increased. To overcome this problem, automobile manufacturers have developed power steering systems (Hydraulic and Electric). The power steering reduces a large amount of driver's physical effort by providing steering assistance. A Hydraulic Power Steering (HPS) system uses hydraulic pressure supplied from an engine driven pump to assist turning of the steering wheel. On the other hand, an electric motor generates steering assistance in electric power steering systems, to make steering more comfortable for drivers.

EPS systems have been gradually used to replace hydraulic power steering in small and medium size vehicles in recent years [1].

The EPS systems are more fuel efficient because the electric motor consumes power only when the steering wheel is turned, but the hydraulic pump in HPS always runs regardless of whether steering assistance is required or not. Briefly, the following points can be mentioned as advantages of EPS over HPS systems: engine independence/fuel economy, tunability of steering feel, modularity/quick assembly, compact size and environmental friendliness [2].

Designing an EPS system requires solving a tracking

control problem under the existence of disturbance and uncertainty. The EPS controller must follow the desired current of motor extracted from a given characteristic curve to reduce steering effort and improve driver steering feel.

Performance criteria in EPS systems such as comfort and feel are subjective matters because they vary according to drivers and driving conditions. Therefore, it is difficult to quantify those using available measurements. To alleviate this, EPS characteristic curves were developed. These curves set the desired amount of additional assistance torque to achieve the appropriate steering feel.

Random road excitation and parameter uncertainty make establishing an exact mathematical model difficult and thus the control problem becomes challenging and important.

There is some research and development on power steering systems, either hydraulic or electric. In [3], different types of EPS systems have been simulated using Newton-Euler mechanics and the effect of applied assistance torque position on performance of EPS is investigated.

In [2] and [4], high-order lead-lag compensator and Proportional Integral Derivative (PID) controllers are successfully implemented. Compensators and PID control algorithms have simple structures and low implementation cost. However, their performances are degraded in the presence of disturbance and uncertainty such as tire forces and friction in the EPS system. In [5], LQG control method for EPS systems is investigated; the control design method employed the characteristic curve to form a LQG feedback control to improve performance, robustness and disturbance rejection properties.

In this paper, first the architecture and principle of EPS is introduced in detail. Then based on the architecture, the dynamic equations and state equations of EPS are built. For this system a new optimal disturbance rejection controller based on stochastic optimal control is proposed, and its performance and robustness is compared to PID and conventional LQG control methods. Finally simulation results are presented and conclusions are made.

## II. DYNAMIC MODEL OF EPS SYSTEM

### A. Architecture and principle of EPS

An EPS system usually consists of a vehicle speed sensor, torque sensor, steering angle sensor, Electronic Control Unit (ECU) and motor as shown in Fig.1.

When a vehicle with EPS system turns, the column torque (measured by torque sensor) and the steering angle are

Manuscript received March 21, 2011.

N. Mehrabi is a PhD candidate in the Department of System Design Engineering at University of Waterloo, Waterloo, ON N2L 3G1 Canada (phone: 519-888-4567 Ext. 37099; e-mail: nmehrabi@uwaterloo.ca).

N. L. Azad is with Department of Systems Design Engineering at University of Waterloo, Waterloo, ON N2L 3G1 Canada (e-mail: nlashgar@uwaterloo.ca).

J. McPhee is with Department of Systems Design Engineering at University of Waterloo, Waterloo, ON N2L 3G1 Canada (e-mail: mcphee@uwaterloo.ca).

detected and are sent to the ECU. The ECU defines target motor current based on the pre-established characteristic curves, steering direction and vehicle speed. Then it regulates the voltage of the electric motor to produce a desired current. The gearbox is used to decrease the motor speed to amplify the assist torque, and finally the loop is closed by applying the magnified torque to the steering column.

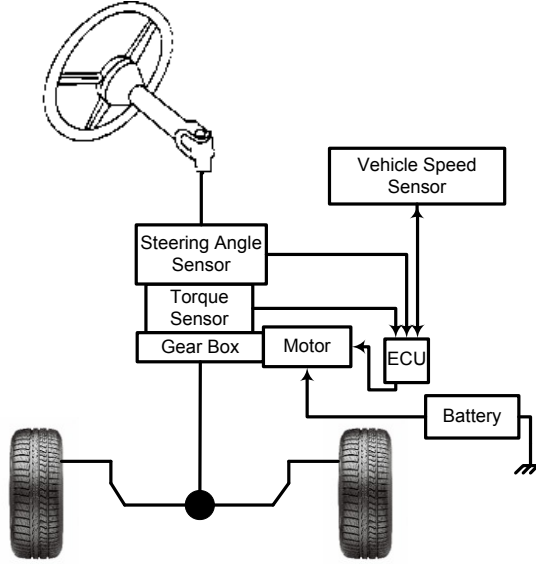


Fig. 1. Architecture of EPS system

### B. Column-assisted electric power steering model

Uncertainties in EPS systems mainly result from road excitation, measurement noise and nonlinear friction characteristics. Therefore, it is impossible to establish an exact dynamic model of EPS system. However, creating an EPS model is a necessary step to study EPS dynamics.

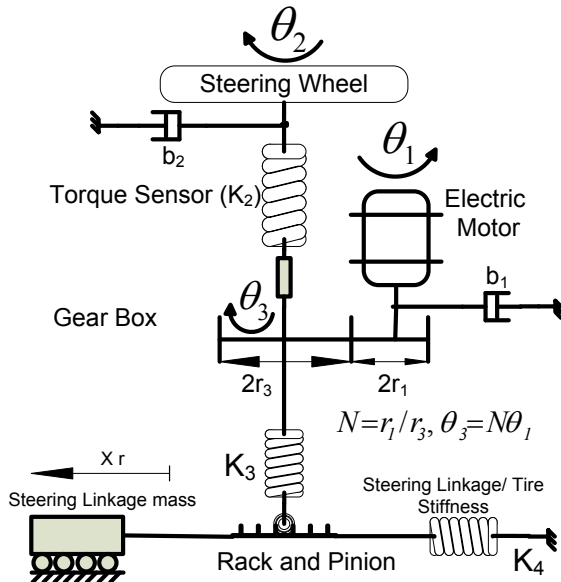


Fig. 2. Column-Type EPS schematic diagram

The major mechanical components of EPS systems are the steering wheel, steering column, electric motor, gearbox and rack. Fig. 2 shows a schematic diagram of a column-type

EPS system.

Newton-Euler equations of motion can be derived to describe dynamics of a column-type EPS system [2]. The dynamic equation of the DC motor and nonlinear friction of the steering column and motor shaft are also added to the original model to provide higher fidelity. Driver torque is applied to the steering system at the steering wheel. The steering wheel is connected to the gearbox via the steering column and torque sensor. Considering the moment of inertia and the viscous damping of input axle, an equation obtained using Newton second law,

$$J_2\ddot{\theta}_2 = u_\tau - K_2(\theta_2 - N\theta_1) - b_2\dot{\theta}_2 + f_1(\dot{\theta}_2) \quad (1)$$

where  $u_\tau$  is driver torque.  $\theta_2$ ,  $J_2$ ,  $K_2$ ,  $b_2$  and  $f_1(\dot{\theta}_2)$  are angle of rotation, moment of inertia, stiffness, viscous damping and nonlinear friction of the steering column.

Electric motor torque is exerted on motor axle at one end, and the axle is connected to reduction gear at the other end. To analyze the motor shaft, an equation can be obtained as follows,

$$J_{eq}\ddot{\theta}_1 = \tau_m + \left[ K_2(\theta_2 - N\theta_1) - K_3 \left( N\theta_1 - \frac{x_r}{r_p} \right) \right] N - b_1\dot{\theta}_1 + f_2(\dot{\theta}_1) \quad (2a)$$

$$J_{eq} = J_1 + N^2 J_3 \quad (2b)$$

where  $\theta_1$ ,  $J_1$ ,  $b_1$  and  $f_2(\dot{\theta}_1)$  are angle of rotation, moment of inertia, viscous damping and nonlinear friction of the electric motor.  $J_3$  and  $K_3$  are gearbox moment of inertia and universal joint stiffness.  $\tau_m$  is assist torque;  $N$ ,  $r_p$  are transmission ratio and pinion radius.

To analyze the rack dynamics, such equation as follows can be obtained,

$$m\ddot{x}_r = \frac{K_3}{r_p} \left( N\theta_1 - \frac{x_r}{r_p} \right) - \frac{K_4}{L_{la}^2} x_r - b_r\dot{x}_r - f_3(\dot{x}_r) - u_d \quad (3)$$

$x_r$ ,  $m$ ,  $K_4$ ,  $b_r$  are rack displacement, mass, stiffness and damping of the rack.  $f_3(\dot{x}_r)$  is rack friction and  $L_{la}$  is steering linkage lever arm.  $u_d$  is the element of tire self-aligning moment (SAM), created by interaction of tire and ground, on the rack.

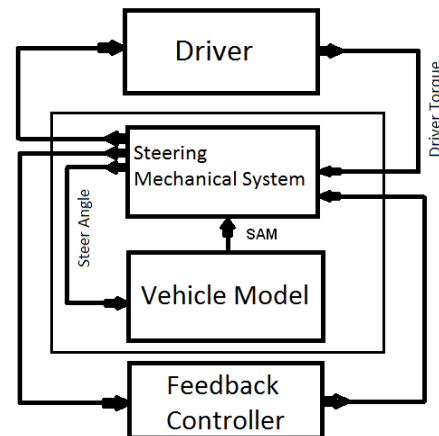


Fig. 3. Schematic diagram of simulation setup

When the vehicle steers, steering resistance primarily is

influenced by the SAM. Vehicle dynamics, road condition and speed of the steering wheel would affect the SAM. To find this signal, a nonlinear 14 degree of freedom vehicle model with Fiala tire model [6] is created. For modeling other minor various disturbances, a random noise is added to this signal. Schematic diagram of the whole simulation setup is shown in Fig. 3.

A DC motor is used to provide the desired assistance torque. Application of Kirchhoff's Voltage Law yields the dynamics of the assist motor as:

$$L_m \dot{i} + R_m i + K_e \dot{\theta}_1 = u_v \quad (4)$$

where  $i$ ,  $u_v$  are current and terminal voltage.  $L_m$ ,  $R_m$  and  $K_e$  are the inductance, resistance and back electromotive force (emf) of the electric motor.

### C. State-Space Formulation

Inputs to the EPS system are driver torque, terminal voltage of electric motor and disturbance force on rack. Based on measurements, outputs are steering wheel angle and steering column torque. The torque sensor is a torsion bar, so the amount of torque twisting the torsion bar is directly proportional to the difference between input and output axle angles, hence column torque is

$$T_s = K_2(\theta_2 - \theta_3) \quad (5)$$

where  $K_2$  is the stiffness of torsion bar and  $\theta_3$  is the angle of the steering column at the reduction gear.

To construct the state-space representation, the state variables of the EPS system are defined as

$$x = [\theta_1 \quad \dot{\theta}_1 \quad \theta_2 \quad \dot{\theta}_2 \quad x_r \quad \dot{x}_r \quad i + aT_0] \quad (6)$$

where  $a$  is the slope of the EPS characteristic curve at each velocity. The characteristic curve shows the relation between the measured torque from the torque sensor and desired current of the electric motor (Fig.4). In this paper, the value of  $aT_0$  is equal to 1 A.

By substitution of each variable into the differential equations of (1) - (4), and omitting nonlinear parts  $f_1(\dot{\theta}_2)$ ,  $f_2(\dot{\theta}_1)$  and  $f_3(\dot{x}_r)$ , the state-space linearized equations of the EPS system can be described by:

$$\begin{aligned} \dot{x}(t) &= Ax(t) + B_\tau u_\tau(t) + B_d u_d(t) + B_u u_v^*(t) \\ y(t) &= Cx(t) + Du(t) \end{aligned} \quad (7)$$

where the system matrix is  $A$ ,  $B_\tau$ ,  $B_d$  and  $B_u$  are input matrices related to driver torque, disturbance and modified terminal voltage ( $u_v^*(t) = u_v(t) + R_m a T_0$ ) and  $C$ ,  $D$  output matrices are,

$$A = \begin{bmatrix} 0 & 1 & 0 & 0 & 0 & 0 & 0 & 0 \\ N^2(K_2 + K_3) & -b_1 & K_2 N & 0 & K_3 N & 0 & K_i & 0 \\ J_{eq} & J_{eq} & J_{eq} & 0 & r_p J_{eq} & 0 & J_{eq} & 0 \\ 0 & 0 & 0 & 1 & 0 & 0 & 0 & 0 \\ K_2 N & 0 & -K_2 & -b_2 & 0 & 0 & 0 & 0 \\ J_2 & 0 & -J_2 & J_2 & 0 & 0 & 0 & 0 \\ 0 & 0 & 0 & 0 & 0 & 1 & 0 & 0 \\ K_3 N & 0 & 0 & 0 & -\frac{K_4/L_a^2 + K_3/r_p^2}{m} & -\frac{b_r}{m} & 0 & 0 \\ m r_p & 0 & 0 & 0 & 0 & 0 & 0 & -\frac{R}{L_m} \\ 0 & -\frac{K_e}{L_m} & 0 & 0 & 0 & 0 & 0 & 0 \end{bmatrix} \quad (8)$$

$$B_\tau = \begin{bmatrix} 0 & 0 & 0 & 1/J_2 & 0 & 0 & 0 \end{bmatrix}^T \quad (9)$$

$$B_d = \begin{bmatrix} 0 & 0 & 0 & 0 & 0 & -1/m & 0 \end{bmatrix}^T \quad (10)$$

$$B_u = \begin{bmatrix} 0 & 0 & 0 & 0 & 0 & 0 & 1/L_m \end{bmatrix}^T \quad (11)$$

$$C = \begin{bmatrix} 0 & 0 & 1 & 0 & 0 & 0 & 0 \\ -K_2 N & 0 & K_2 & 0 & 0 & 0 & 0 \end{bmatrix} \quad (12)$$

$$D = [0]_{2 \times 3} \quad (13)$$

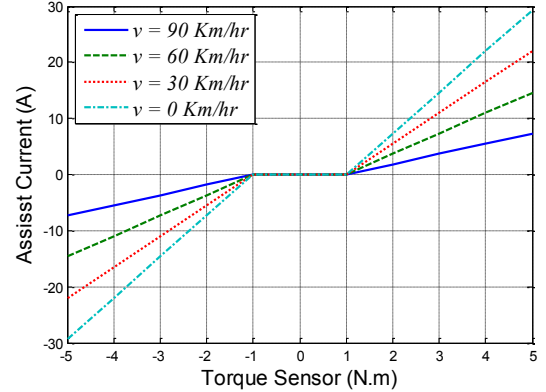


Fig. 4. EPS characteristic curves

### III. CONTROL

In this paper, three different control strategies are implemented on the EPS system. Performance, stability and robustness of these methods are investigated. These methods are PID, LQG and modified LQG.

The aim of the EPS controller is to follow the target assist current of the motor. The target assist current is derived from characteristic curves (Fig.4) using vehicle velocity ( $v$ ) and steering torque measured by torque sensor ( $T_s$ ).

First, a classic PID control method is implemented. This control method needs torque sensor, vehicle speed and motor current signals. Depending on the first two signals and pre-established assist torque curves, the target current of the electric motor is defined. The difference between target current and feedback current measurements feeds into a PID control algorithm to reduce the error.

The second investigated method is the LQG control method. Model-based controls are now accepted by the automotive industry as an effective approach to achieve complex objectives such as improved driver feel and reduced effort, simultaneously. This approach compared with static rule-based control has better performance in the transient response of vehicle operations. However, challenges are still posed in practical applications.

The EPS system is subjected to two external inputs in the form of driver torque and friction force from the road. The steering characteristic curve shown in Fig.4 includes two intervals:  $[0, T_0]$  is the interval with no steering assistance,  $[T_0, T_{max}]$  is the interval with linear steering assistance. Therefore, for full tracking of characteristic curves in the whole operating region two control laws are needed. First law is to control current of the electric motor to be zero and

the second law is to control assist current proportional to the torque measured by torque sensor.

The EPS dynamic equations (7) can be written by forming a disturbance vector  $\kappa$  including  $u_\tau$  and  $u_d$  which are driver torque and disturbance force generated from road-tire interaction respectively. Therefore, the dynamics of the system can be described by

$$\dot{x} = Ax + B_u u_v^* + \begin{bmatrix} B_\tau & B_d \end{bmatrix} \kappa \quad (14)$$

Following cost function is proposed for the first interval:

$$J_0 = \int_0^\infty \left( q i^2 + \rho u_v^2 \right) dt \quad (15a)$$

The cost function for the second interval is [5]:

$$\begin{aligned} J_1 &= \int_0^\infty \left( q (i - i_m)^2 + \rho u_v^{*2} \right) dt \\ &= \int_0^\infty \left( q (x_7 - aK_2(x_3 - Nx_1))^2 + \rho u_v^{*2} \right) dt \end{aligned} \quad (15b)$$

Here,  $i$  and  $i_m$  are actual and desired current and  $u_v$  is the terminal voltage of the electric motor. The weights of current error ( $q$ ) and terminal voltage ( $\rho$ ) in cost functions  $J_0$  and  $J_1$  are chosen by trial and error to ensure that the current of electric motor will track the desired current with minimum electric motor terminal voltage. Therefore, the cost function in its standard integral quadratic form is described by,

$$J_1 = \int_0^\infty \left( x Q x^T + u_v^* R u_v^{*T} \right) dt \quad (16)$$

where

$$Q = \begin{bmatrix} a^2 K_2^2 N^2 q & 0 & -a^2 K_2^2 N q & 0 & 0 & 0 & -a K_2 N q \\ 0 & 0 & 0 & 0 & 0 & 0 & 0 \\ -a^2 K_2^2 N q & 0 & a K_2^2 q & 0 & 0 & 0 & -q a K_2 \\ 0 & 0 & 0 & 0 & 0 & 0 & 0 \\ 0 & 0 & 0 & 0 & 0 & 0 & 0 \\ 0 & 0 & 0 & 0 & 0 & 0 & 0 \\ -a K_2 N q & 0 & -q a K_2 & 0 & 0 & 0 & q \end{bmatrix}, R = \rho \quad (17)$$

It can be shown [7] that the optimal controller is a full state feedback controller, and the optimal law is given by

$$u_v^*(t) = K_{FB} x(t) \quad (18)$$

where

$$K_{FB} = -R^{-1} B_u^T S \quad (19)$$

Here,  $S$  is the solution to the appropriate Riccati equation.

However, the practical implementation of the optimal controller requires the measurement of all state variables. This is a serious limitation because of difficulties involved in measurement of all states. One solution is to construct unavailable states from the available measurements. In this paper, according to state equations of system, a Kalman Filter is used as an optimal state estimator as follows [7]:

$$\dot{\hat{x}} = \hat{A} \hat{x} + \hat{B}_u u_v^* + L(y - \hat{C} \hat{x}) \quad (20)$$

where  $\hat{x}$  is estimation of state variables,  $\hat{A}$ ,  $\hat{B}_u$  and  $\hat{C}$  are nominal value of  $A$ ,  $B_u$  and  $C$  matrices.  $L$  is observer gain which is given by

$$L = -PC^T R^{-1} \quad (21)$$

where  $P$  is the solution to the appropriate Riccati equation.

It can be shown by using the separation principle the optimal input control can be determined by feeding estimated states instead of measurements into eq.(18). Then the optimal feedback control becomes:

$$u_v^*(t) = K_{FB} \hat{x}(t) \quad (22)$$

Here,  $K_{FB}$  is the same gain array obtained from optimal feedback.

As shown in the next section, although it seems the LQG control method has good tracking properties, its performance is degraded outside of nominal conditions. To overcome this, the LQG control is modified for optimal disturbance rejection. The modified LQG controller can make the EPS insensitive to parameter variations and disturbances. It also gives the EPS system good robustness properties.

Effective disturbance rejection can be achieved if the dynamic properties of the disturbance are modeled and included in the controller design [8, 9].

It is possible to optimize a controller for a specific maneuver with particular inputs, but in reality the vehicle is subjected to a range of different inputs which may or may not match the assumed maneuver. A good controller must be optimized over a range of maneuvers.

The steering torque ( $u_\tau$ ) and disturbance force ( $u_d$ ) can be modeled as zero-mean colored stochastic processes. It is often convenient to model a random process as the result of a linear filtering operation on stationary white noise. While it is not possible to predict the exact value of a random process, it is possible to describe its typical frequency content in the form of a power spectral density function.

The driver torque input can be modeled using shaping filter ( $A_{D1}$ ,  $B_{D1}$ ,  $C_{D1}$ ,  $D_{D1}$ ). The shaping filter transforms white noise  $w$  into appropriately stationary random process of driver torque.

$$\dot{x}_{D1} = A_{D1} x_{D1} + B_{D1} w \quad (23a)$$

$$u_\tau = C_{D1} x_{D1} + D_{D1} w \quad (23b)$$

Same for road force friction, a shaping filter ( $A_{D2}$ ,  $B_{D2}$ ,  $C_{D2}$ ,  $D_{D2}$ ) is used such that a zero-mean white noise source  $w$  at the input produces an appropriately time correlated stochastic friction disturbance at the output:

$$\dot{x}_{D2} = A_{D2} x_{D2} + B_{D2} w \quad (24a)$$

$$u_d = C_{D2} x_{D2} + D_{D2} w \quad (24b)$$

where  $x_{D1}$  and  $x_{D2}$  are disturbance states. Note that the shaping filter corresponding to (23) and (24) are causal first order low-pass filters with  $D_D = 0$ .

Driver torque and friction force act on the steering system based on matrices  $B_\tau$  and  $B_d$ . By substitution of (23b) and (24b) into (7), dynamics of the system is described by

$$\begin{aligned} \dot{x} &= Ax + B_u u_v^* + B_\tau u_\tau + B_d u_d \\ &= Ax + B_u u_v^* + B_\tau C_{D1} x_{D1} + B_\tau D_{D1} w \\ &\quad + B_d C_{D2} x_{D2} + B_d D_{D2} w \end{aligned} \quad (25)$$

Equation (25) can be rewritten by forming an augmented state vector  $\underline{x}$  including the system states  $\mathbf{x}$  and the disturbance state  $x_{D1}$  and  $x_{D2}$  such that the dynamics of the system are described by

$$\dot{\underline{x}} = \underline{A}\underline{x} + \underline{B}_u u_v^* + \underline{B}_w w \quad (26)$$

where

$$\underline{x} = \begin{bmatrix} \mathbf{x} \\ x_{D1} \\ x_{D2} \end{bmatrix}, \quad \underline{A} = \begin{bmatrix} A & B_\tau C_{D1} & B_d C_{D2} \\ 0 & A_{D1} & 0 \\ 0 & 0 & A_{D2} \end{bmatrix}, \quad (27)$$

$$\underline{B}_u = \begin{bmatrix} B_u \\ 0 \\ 0 \end{bmatrix}, \quad \underline{B}_w = \begin{bmatrix} B_\tau D_{D1} + B_d D_{D2} \\ B_{D1} \\ B_{D2} \end{bmatrix}$$

The optimal control is chosen to minimize the performance index described in equation (16). Regarding changes in number of state variables, the  $Q$  and  $R$  matrices are changed as follows

$$Q = \begin{bmatrix} Q & 0 & 0 \\ 0 & 0 & 0 \\ 0 & 0 & 0 \end{bmatrix} \quad (28)$$

$$R = \rho$$

The optimal controller is a full state feedback controller operating on  $\underline{x}$ , and the optimal law is given by

$$u_v^*(t) = \underline{K}_{FB} \underline{x}(t) \quad (29)$$

where

$$\underline{K}_{FB} = -R^{-1} \underline{B}_u^T S \quad (31)$$

where  $S$  is the solution to the appropriate Riccati equation.

#### IV. SIMULATION

In the simulation, the full nonlinear vehicle model is used and the vehicle speed ( $v$ ) and assist gain ( $a$ ) are set to 60 km/hr and 3.6595 A/N.m, the driver command is a steering wheel torque signal which begins at zero, goes to -2 N.m, then it goes to 2 N.m and finally returns to zero. Response curves of motor current as a function of column torque  $T_s$  are shown in Fig. 5, where the solid curve is the EPS characteristic curve and dotted lines were simulation results for the designed PID and LQG controllers.

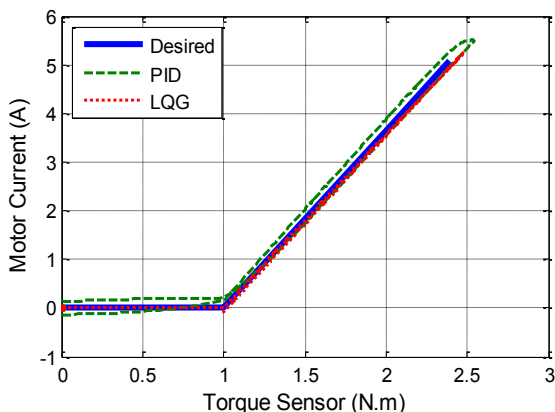


Fig. 5. Ramp input response curves of assist current/Torque (The curves are symmetric about the origin).

As shown in Fig.5, the LQG control method has an advantage over PID control in respect of performance. Furthermore, simulation investigation shows that PID control is unstable at high assist gains[10]. Although LQG control has better performance and stability robustness properties than PID control, its tracking performance decreases outside of nominal conditions.

Fig. 6 shows the response of the LQG-controlled EPS system with changes of system parameters. In these simulations the damping coefficient of the column and steering wheel are scaled using a common constant gain  $\alpha$ . As shown, the performance of the EPS system is degraded by reducing the gain  $\alpha$ .

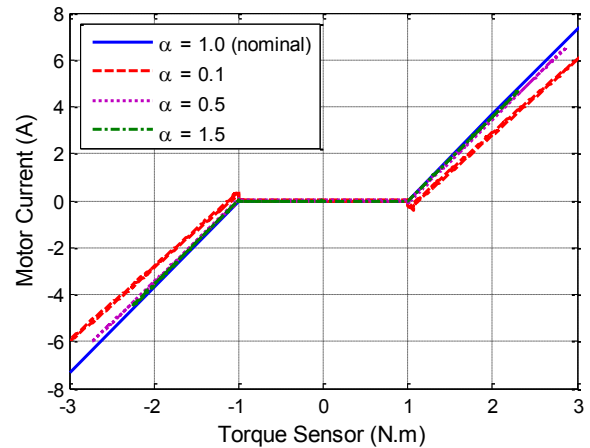


Fig. 6. Ramp input response of the LQG control with changed parameters

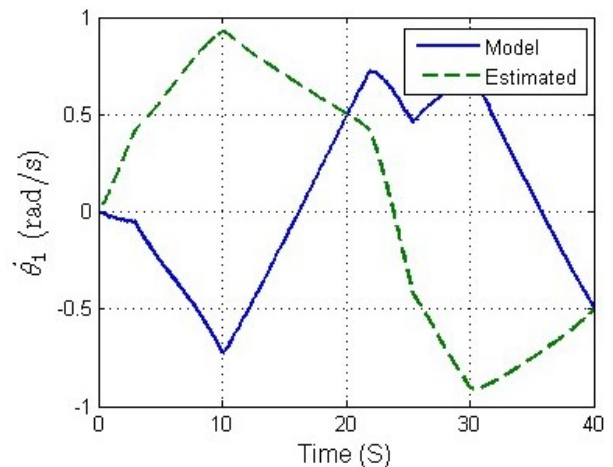


Fig. 7. Estimated and actual values of  $\theta_1$

Due to performance degradation, the accuracy of state variable estimation is investigated. Fig. 7 and Fig. 8 show the observer is not able to estimate all state variables accurately in the presence of two exogenous inputs.

As shown in Fig. 9, the behavior of the modified LQG control method is improved in respect of changes in system parameters. The controller can track the EPS characteristic curve precisely even when column and steering wheel damping coefficients changed significantly.

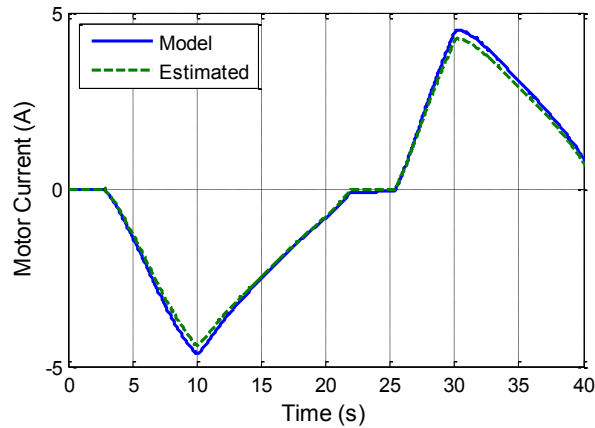


Fig. 8. Estimated and actual values of electric motor current

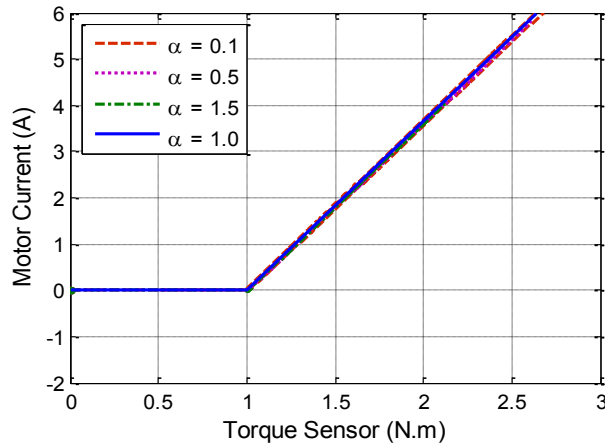


Fig. 9. Ramp input response of the Modified LQG control with changed parameters (The curves are symmetric about the origin).

To study performance of this algorithm with high assist gains, several simulations were carried out with different gain values. As it is shown in Fig.10, the modified LQG control works well with high assist gains.

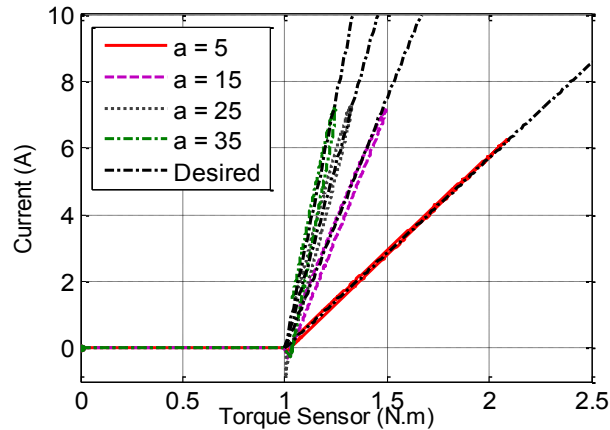


Fig. 10. Modified LQG response with high gain assists (The curves are symmetric about the origin).

## V. CONCLUSION

In this paper, three different EPS control methods were investigated. The PID control has satisfactory performance but it becomes unstable at high assist gains. The LQG control has better performance but its performance decreases

when system parameters change.

The Modified LQG controller designed in this paper has strong robustness which can efficiently attenuate the interference caused by road random excitation, torque sensor measurement noise and model parameter uncertainty, and can strengthen the anti-interference ability of the EPS system. Through simulation, we can choose a weight of assist current error that minimizes the energy consumption and the error between actual assist current of motor and target assist current of motor.

## APPENDIX

Nominal parameter values used in the computer simulations are :

TABLE I  
NOMINAL PARAMETERS VALUES

Parameters	Symbols/Value
Electric motor moment of inertia	$J_1=1.947 (kg\ cm^2)$
Steering wheel moment of inertia	$J_2=3.3 (kg\ cm^2)$
Gearbox moment of inertia	$J_3=1 (kg\ cm^2)$
Torsion bar stiffness	$K_2=120 (N\ m/rad)$
Universal joint stiffness	$K_3=3277 (N\ m/rad)$
Steering linkage stiffness	$K_4=1800 (N\ m/rad)$
Electric motor viscous damping	$b_1=0.01 (N\ m\ s)$
Steering column viscous damping	$b_2=1.265 (N\ m\ s)$
Rack viscous damping	$b_r=163 (N\ s/m)$
Rack mass	$m=6.8 (kg)$
Steering linkage lever arm	$L_{ia}=0.3 (m)$
Pinion radius	$R_p=0.8 (cm)$
Transmission ratio	$N=1/18.5$
Electric motor emf constant	$K_e=0.5 (V/(rad/s))$
Electric motor resistance constant	$R_m=0.373 (ohm)$
Electric motor inductance constant	$L_m=0.0127 (H)$

## REFERENCES

- [1] X. Chen. Control-Oriented Model for Electric Power Steering System. SAE Technical Paper, 2006-01-0938, Detroit, Michigan, 2006.
- [2] A. H. El-Shaer. Robust Control Design of Electric Power Steering Systems. Dept. of Mech. Engr. UC Berkeley PhD thesis, 2008.
- [3] H. Mohammadi and R. Kazemi. Simulation of Different Types of Electric Power Assisted Steering (EPS) to Investigate Applied Torque Positions' Effects. SAE Technical Paper, 2003-01-0585, Detroit, Michigan, 2003.
- [4] A. Zaremba, M. Liubakka, and R. M. Stuntz. Vibration Control based on Dynamic Compensation in an Electric Power Steering System. In Control and Decision Conference, St. Petersburg, Russia, 1997.
- [5] P. Shi, S. Gao and L.Miao. Optimal Controller Design for Electric Power Steering System Based on LQG, Information Engineering and Computer Science, 2009. ICIECS 2009. International Conference on, pp.1-4, 19-20 Dec. 2009.
- [6] MSC. ADAMS online help, ADAMS/Tire, 2003.
- [7] D. Kirk, Optimal Control Theory, Prentice-Hall, Englewood Cliffs, 1970.
- [8] C. F. Lin. Advanced Control Systems Design. Prentice Hall, Upper Saddle River, NJ, USA, 1994.
- [9] D. J. M. Sampson, Active Roll Control of Articulated Heavy Vehicles, Ph.D. Thesis, University of Cambridge, UK, 2000.
- [10] A. Zamerba, R. I. Davis. Dynamic Analysis and Stability of a Power Assist Steering System, In American Control Conference, Seattle, Washington, 1996.